International Journal of Applied Pharmaceutics

ISSN- 0975-7058 Vol 15, Issue 5, 2023

Original Article

FIXED DOSE COMBINATION THERAPY OF IBRUTINIB AND QUERCETIN BY SNEDDS-DEVELOPMENT AND EVALUATION BY DESIGN OF EXPERIMENT

RASHMI BAGRI[1,2*], RAVOURU NAGARAJU[2]

[1]Malla Reddy Pharmacy College, Maisammaguda, Secunderabad-500100, Telangana, India. [2]Institute of Pharmaceutical Technology, Sri Padmavati Mahila Visvavidyalayam (Women's University), Tirupati-517502, Andhra Pradesh, India
[*]Corresponding author: Rashmi Bagri; [*]Email: rashmi.hsg1@gmail.com

Received: 13 Mar 2023, Revised and Accepted: 05 Aug 2023

ABSTRACT

Objective: Self-nano emulsifying drug delivery system (SNEDDS) comprising quercetin and ibrutinib as a fixed dosage combination therapy is being investigated to increase drug solubility and dissolution rate.

Methods: On the basis of preliminary solubility tests, castor oil, Kolliphor® RH 40, and PEG600 were utilised to construct ternary phase diagrams. The effect of the amount of Castor oil (A), Kolliphor® RH 40 (B), and PEG600 (C) on the particle size and encapsulation efficiency of ibrutinib and quercetin was evaluated and statistically analysed using multiple regression in 17 trials planned using a 33 Box-Behnken design. FTIR, XRD, DSC, SEM, and stability experiments were employed to characterise the optimised formulation. The particle size, zeta potential, polydispersity index, encapsulation efficiency, and *in vitro* drug release of ibrutinib and quercetin were also investigated.

Results: Ibrutinib and quercetin had encapsulation efficiencies of 61.56-87.22% (Y3) and 60.12-87.12%, respectively, according to the size range of SNEDDS formulations (1-17) of 70.18-200.56 nm. The optimised SNEDDS formulations (S1–S3) showed a particle size range of 71.12–76.38 nm, PDI of 0.126–0.312, zetapotential of-24.6–28.4, and encapsulation efficiencies of 88.98–90.22% and 84.96–86.78% for ibrutinib and quercetin, respectively. According to *in vitro* testing, the medication released from SNEDDS was released more quickly (>90% 600 min). The formulation was further evaluated using FTIR, XRD, DSC, SEM, and stability investigations, which validated the complexation of ibrutinib and quercetin in the drug's amorphous state and stability for six months.

Conclusion: This study revealed that SNEDDS could be used as a drug carrier for ibrutinib and quercetin due to their improved solubility and dissolution rate.

Keywords: Ibrutinib, Quercetin, Box behnken design, Solubility, SNEDD

DOI: https://dx.doi.org/10.22159/ijap.2023v15i5.47820. Journal homepage: https://innovareacademics.in/journals/index.php/ijap

INTRODUCTION

The simultaneous modulation of various cell-signaling mechanisms through multimodal chemotherapy is considered a vital protocol for enhancing therapeutic efficacy and reducing systemic toxicity. In recent years, the utilization of nanocarriers for delivering a combination of chemotherapeutic medications has emerged as a promising approach in cancer treatment [1]. Co-delivery systems offer a solution to the challenges associated with poor solubility and stability of certain drugs. These systems enable simultaneous transportation of multiple medications to the intended site, controlled release of the payloads in precise doses, synchronization of drug exposure, maximization of therapeutic efficacy, and minimization of toxicity [2]. The concurrent administration of antioxidants with anti-proliferative properties, along with their inherent antioxidant capabilities, holds significant potential for enhancing the overall effectiveness of antitumor treatments while reducing the toxicity associated with anticancer medications. In our study, we specifically aim to investigate the combination of two medications, namely Ibrutinib and quercetin. By studying the therapeutic effects of this medication combination, we hope to gain insights into how the synergistic interaction between these compounds can lead to improved antitumor outcomes and reduced side effects [3].

Ibrutinib is used to treat B-cell malignancies because it is a specific and covalent inhibitor of the Bruton's tyrosine kinase (BTK) enzyme [4]. Ibrutinib has a pKa of 3.74, making it a weak base. It is essentially insoluble in water (mole fraction solubility: 1.43 x 10-7 at room temperature), easily soluble in dimethyl sulfoxide, soluble in methanol, and has a very limited oral bioavailability (2.9%).

Quercetin is a polyphenolic flavonoid molecule that has been shown to have a number of potential biological actions. Some of these activities include the activation of apoptosis, the prevention of angiogenesis, and an anti-proliferative effect on a number of human cancer cells.

There are a few different approaches that may be taken in order to improve the bioavailability of anticancer drugs and ensure that they are effectively delivered. Some of these technologies include lipid-based delivery systems, polymeric nanoparticulate systems, crystal engineering (nanocrystals technology, co-crystal technology), liquisolid technology, self-emulsifying solid dispersions, and P-efflux inhibition strategies [5].

When a synthetic or natural oil, a surfactant, and a co-surfactant are introduced to an aqueous phase while being gently stirred, they produce a fine oil-in-water nanoemulsion that is known as a SNEDDS. SNEDDS are multi-component drug delivery systems that are isotropic. In addition to enhancing solubility and dissolving, researchers have been looking at the effects that SNEDDS have on increasing permeability, the hepatic first-pass effect, and bypassing the P-glycoproteins efflux [6].

In the area of formulation development, the Design of Experiment method has seen significant growth in popularity during the past several years [7]. In the present study, we have chosen the self-nano-emulsifying drug delivery system (SNEDDS) as the preferred method for delivering the proposed combination therapy of ibrutinib and quercetin. SNEDDS is a promising drug delivery system known for its ability to enhance the solubility, bioavailability, and therapeutic efficacy of poorly soluble drugs. By using SNEDDS, we aim to overcome the challenges associated with the limited solubility of ibrutinib and quercetin, ensuring their efficient delivery to the target site. The utilization of SNEDDS as a drug delivery method in our combination therapy approach holds the potential for achieving enhanced treatment outcomes and promoting the clinical translation of ibrutinib and quercetin as an effective therapeutic option. All of the ingredients used to make SNEDDS are nontoxic and fall into the category of excipients that are widely recognised as safe. Utilizing a 3-factor, 2-level Box Behnken design, the SNEDDS were optimised (BBD).

MATERIALS AND METHODS

Materials

The following materials were obtained from the indicated sources and used without further purification. Ibrutinib was purchased from Hetero Drugs Ltd., Hyderabad, India, and Quercetin was obtained from Research-Lab Fine Chem Industries, Mumbai, India. Linseed oil, olive oil, castor oil, sesame oil, groundnut oil, soyabean oil, Kolliphor® RH 40, and Kolliphor® EL were purchased from MSN Labs, Hyderabad, India. Tween-80, Tween-20, Span-80, Span-20, Carbitol, Triton X-100, PEG-300, PEG-400, PEG-600, Polypropylene glycol, Ethanol, Methanol, and Milli Q water were purchased from SD Fine Chemical Ltd., Mumbai.

Development of a UV-spectrophotometric method for the simultaneous estimation of ibrutinib and quercetin

Preparation of standard stock solution and calibration curve

The two drugs, ibrutinib and quercetin, showed good absorbance when dissolved in methanol. Hence, methanol was selected as the solvent for this method. Ibrutinib and quercetin (10 mg each) were separately weighed and transferred to a 100ml volumetric flask, and the two drugs were dissolved in methanol to get a solution of 100 µg/ml of standard stock solution. Working standard solutions of 10 µg/ml were scanned in the entire UV range of 400–200 nm to determine the λmax. The λmax of ibrutinib and quercetin is 277 nm and 256 nm, respectively, from the overlain spectra. Five working standard solutions (2, 4, 6, 8, and 10 µg/ml) for each drug were prepared in methanol from stock solution. To obtain the linearity and regression equations, the absorbance's of the resulting solutions were measured at their respective maximums and plotted on a calibration curve.

Two wavelengths, namely 277 nm and 256 nm, were selected, which are the λmax of two drugs, ibrutinib and quercetin, respectively. At 277 nm and 256 nm, the absorptivity of these two drugs was measured. Equations 1 and 2 were used in tandem to compute the concentrations of the two drugs in the mixture:

$$C_x = A_2\, ay_1 - A_1\, ay_2 / ax_2\, ay_1 - ax_1\, ay_2 \ldots. \quad (1)$$

$$C_y = A_1\, ax_2 - A_2\, ax_1 / ax_2\, ay_1 - ax_1\, ay_2 \ldots. (2)$$

Where C_x and C_y are the ibrutinib and quercetin concentrations (µg/ml) in the known sample solution. A_1 and A_2 are the absorbances of the sample solution at 277 nm and 256 nm, respectively. Ibrutinib's absorptivity at 277 nm and 256 nm is represented by a_{x1} and a_{x2}, whereas quercetin's absorptivity is represented by a_{y1} and a_{y2}.

Saturation solubility studies-selection of oil

Various oils, surfactants and co-surfactants were screened for their ability to dissolve ibrutinib procedure reported elsewhere [8].

Preliminary screening of surfactant and co-surfactant

Based on the solubility study results, two each of surfactants and co-surfactants were selected for the emulsification study reported elsewhere [9]. The obtained emulsions were kept aside for 2 h and percent transmittance was measured at 638.2 nm using a UV-spectrophotometer against distilled water as blank.

Construction of Pseudo ternary phase diagram

Based on the results of the solubility study and the emulsification tendency, Castor oil, Kolliphor® RH 40 and PEG-600 were selected as oil, surfactant and co-surfactant, respectively. To identify the self-nano emulsifying region, ternary diagrams of oil, surfactant, and co-surfactant were prepared, each representing the apex of the triangle. A visual test method reported by Craig *et al.* was modified and used in the study [10]. Ternary mixtures with varying compositions of oil, surfactant, and co-surfactant were prepared. The oil composition was varied from 40 % w/w to 80 % w/w, surfactant concentration was varied from 20% w/w to 60% w/w, and the co-surfactant concentration was varied from 0 % w/w to 20 % w/w. For all mixtures, the total of oil, surfactant, and co-surfactant was always 100%. The extreme and middle levels of the independent variables, consisting of the oil, surfactant, and co-surfactant, were selected for further study [11, 12].

Optimization of the SNEDDS by experimental design

Box–behnken experiment design

Table a and 2 shows 17 randomized experimental runs for the selected independent variables, including five replicates at the centre point (asterisk-marked) generated from a three-factor, three-level BBD and their corresponding responses [13]. A three-factor, three-level Box-Behnken Design was used for constructing the models with Design Expert® software (Version 8.0, Stat-Ease Inc., Silicon Valley, CA, USA). To explore and optimize the main, quadratic and interaction effects of the formulation ingredients on the performance of the SNEDDS. To determine the experimental error and the precision of the design, according to the three-factor and three-level design, BBD requires 17 randomized experimental runs with six replicates at the centre point. The percentages of independent variables, i.e., percentage of the oil phase (castor oil; X_1; 50–58%), surfactant (Kolliphor® RH 40; X_2; 22–38%), and co-surfactant (PEG-600; X_3; 12–18%), were chosen based on the results obtained from the phase diagram. Droplet size (Y_1), ibrutinib encapsulation efficiency (Y_2), and quercetin encapsulation efficiency (Y_3) were the main response variables utilized to evaluate the quality of the SNEDDS formulation (table 1). The second-order quadratic or polynomial equation can be approximated by the following mathematical model:

$$Y = \beta_0 + \beta_1 X_1 + \beta_2 X_2 + \beta_3 X_3 + \beta_4 X_1 X_2 + \beta_5 X_2 X_3 + \beta_6 X_1 X_3 + \beta_7 X_1^2 + \beta_8 X_2^2 + \beta_9 X_3^2 \ldots\ldots (3)$$

Where Y is the level of the measured response, β_0 is the intercept, β_1 to β_9 are the regression coefficients, X_1, X_2, and X_3 stand for the main effects; X_1X_2, X_2X_3, and X_1X_3 represent the interaction between the main effects; and X_1^2, X_2^2 and X_3^2 are the quadratic terms of the independent variables that were used to simulate the curvature of the designed sample space. The models were validated by lack of fit, ANOVA, and multiple correlation coefficient (R^2) tests.

Optimization using the desirability function

In the present study, all three responses were simultaneously optimized by a desirability function that uses the numerical optimization method introduced by Derringer and Such in the design-expert software (Version 8.0, Stat-Ease Inc., Silicon Valley, CA, USA) [14].

Table 1: List of dependent and independent variables in the inbox-behnken design

Independent variables			**Levels**		
Variable	**Name**	**Units**	**Low (-1)**	**Middle (0)**	**High (+1)**
A	Amount of castor oil	mg	54	57	60
B	Amount of Kolliphor® RH 40	mg	24	30	36
C	Amount of PEG-600	mg	10	15	20
Dependent variable			**Goal**		
Y1	Droplet size	Nm	Minimize		
Y2	Encapsulation efficiency of ibrutinib	%	Maximize		
Y3	Encapsulation efficiency of quercetin	%	Maximize		

Table 2: Box behnken design with observed responses

Run	Amount of castor oil (mg)	Amount of Kolliphor® RH 40 (mg)	Amount of PEG-600 (mg)	Droplet size (nm)	Encapsulation efficiency of ibrutinib (%)	Encapsulation efficiency of quercetin (%)
1	54	24	15	128.82	63.48	60.12
2	60	24	15	189.92	61.56	63.12
3	54	36	15	118.85	80.23	79.18
4	60	36	15	176.89	70.12	65.56
5	54	30	10	138.82	72.48	73.12
6	60	30	10	200.56	69.92	67.78
7	54	30	20	88.53	85.68	83.59
8	60	30	20	148.56	75.66	78.78
9	57	24	10	133.89	65.34	64.89
10	57	36	10	108.26	82.84	79.12
11	57	24	20	70.18	80.58	79.28
12	57	36	20	71.84	86.38	87.12
13	57	30	15	77.86	87.22	85.76
14	57	30	15	79.58	86.12	86.14
15	57	30	15	76.88	85.26	85.98
16	57	30	15	78.12	86.78	86.38
17	57	30	15	76.54	84.42	87.12

Preparation of plain SNEDDS (Placebo formulation)

SNEDDS formulation was prepared by mixing the components in optimized concentrations (Castor oil, Kolliphor® RH 40 and PEG-600) by stirring, vortex mixing and heating at 37 °C on a magnetic stirrer.

Preparation of ibrutinib-quercetin loaded SNEDDS

Drug-loaded SNEDDS formulation was prepared by dissolving specified quantities of both drugs in the mixture of Castor oil, Kolliphor® RH 40and PEG-600. The components were mixed by stirring, vortex mixing and heating at 37 °C on a magnetic stirrer, until both the drugs were dissolved completely. The SNEDDS formulations were stored at room temperature for further studies.

Physicochemical characterization of ibrutinib, quercetin and SNEEDs formulation

Determination of melting point

Ibrutinib and quercetin melting points were determined using the open capillary tube method on the melting point apparatus (MP30, Mettler Toledo with LabXTM software). The procedure was carried out in triplicate.

Differential scanning calorimetry (DSC)

DSC is one of the basic techniques used to determine the purity of drugs and investigate drug-excipient compatibility. The steps involve taking around 5 mg of each sample, sealing it in a DSC aluminum pan, and heating the sample at a rate of 10 °C per minute at a temperature range of 30-400 °C. As a reference standard, an empty aluminum pan was used. Five milligram's of samples were subjected to analyses in triplicate while being nitrogen-purged. The thermograms for pure ibrutinib, quercetin, and the SNEDD formulation were obtained using a DSC instrument (DSC-60 Shimadzu, Japan).

Fourier-transformed infrared (FTIR) spectroscopy

The physicochemical compatibility between ibrutinib, quercetin, and the excipient used to prepare SNEDDS was studied using FTIR (FTIR-8400, Shimadzu, Japan) spectroscopy. The spectra were recorded in the wavelength region between 400 cm^{-1} and 4000 cm^{-1}.

X-Ray powder diffraction study (XRPD)

Powder X-ray diffraction patterns of ibrutinib and quercetin, SNEEDS formulation were traced employing XRD (XRD 7000, Shimadzu, Japan). An X-ray diffractometer with Ni-filtered CuK radiation, a voltage of 40 KV, and a current of 30 mA, radiation scattered in the crystalline portions of the sample. At ambient temperature, XRD patterns were obtained using a step width of 0.04 °C and a detector resolution of 2θ (diffraction angle) between 10° and 80°.

Scanning electron microscopy (SEM)

Scanning electron microscopy (JEM-2000 EXII; JEOL, Tokyo, Japan) was used to observe the SNEDDS formulation's morphology. A film-coated copper grid was coated with a drop of diluted emulsion, which was then stained with a drop of 2% (w/v) phosphotungstic acid aqueous solution before being allowed to dry for contrast enhancement. The samples were examined under Scanning electron microscopy at a magnification of 72,000x.

Determination of droplet size and zeta potential

The mean droplet sizes and polydispersity index of the globules were analyzed using dynamic light scattering with a scattering angle of 90 ° using Mastersizer 2000 (Malvern Instruments Ltd., Worcestershire, UK) equipped with MAS OPTION particle sizing software. Zeta potential measurements were also made using an additional electrode in the same instrument.

Thermodynamic stability studies

Under varied stress conditions, six cooling (4 °C) and heating (40 °C) cycles, as well as freeze-thaw cycles (-21 °C and 25 °C), were used to test the prepared SNEDDS formulations thermodynamic stability. These cycles were carried out for at least 48 h. The stable formulation was tested for centrifugation, which involved centrifuging the formulations for 30 min at 3500 rpm and checking for any phase separation visually [15]. Within 2-3 min, the thermodynamically stable nano-emulsions regained their original form, and they were chosen for further investigation.

Accelerated stability study

The ICH guidelines Q1A (R2) for stability testing were followed when conducting accelerated stability studies. The optimized formulations were stored in a temperature and humidity-controlled stability chamber for three months at 40 °C and 75% RH. Before and after accelerated stability studies, the formulations droplet size, zeta potential, and PDI were measured.

***In vitro* dissolution studies**

The USP type II apparatus (paddle type; Electrolab, TD L8, Mumbai, India) was used for the relative *in vitro* dissolution studies under sink conditions, with the paddle rotating at a speed of 50 rpm. 500 ml of dissolution medium (simulated gastric fluid, pH 1.2), which had been equilibrated at 37 °C, had samples of SNEDDs and individual drug suspensions comprising 10 mg of each drug added to it. In order to maintain a consistent volume of dissolution medium, an aliquot of 5 ml was removed and reintroduced at specified time periods of 5, 10, 15, 30, 45, 60, 90, and 120 min. All samples were filtered and properly diluted, and their drug concentrations were measured using a UV spectrophotometer. 250 ml of 0.3 M dibasic sodium phosphate was added to the dissolution medium after two

hours to change the pH and mimic the gut pH (SIF, pH 6.8). The samples were collected on a regular basis and examined as previously described. There were three triplicates of each measurement.

Kinetic analysis

The data from the *in vitro* release study were fitted into different kinetic models, such as the zero-order, first-order, Higuchi's, and Korsemeyer Peppa's models, to understand the mode and mechanism of drug release. By using the curve fitting method, the release of both drugs from the SNEDDS formulation was calculated. Several kinetic equations were fitted to the data from *in vitro* release studies.

RESULTS AND DISCUSSION

Solubility study

Out of different oils screened; castor oil has a maximum solubility of ibrutinib (3456.28 µg/ml±216.78) and quercetin (2897.93 µg/ml±188.76). Among surfactants and co-surfactants, Kolliphor® RH 40 (9789.28±786.42 µg/ml), kolliphor® EL (7126.678±342.76 µg/ml), tween-80 (6472.82±538.42 µg/ml) and PEG-600 (5973.08±212.32 µg/ml) could solubilize maximum amount of ibrutinib, respectively. For quercetin, Kolliphor® RH 40 (8734.64±423.66 µg/ml) and PEG-600 (7144.85±618.25 µg/ml) provided the highest solubility potential (fig. 1). These results are correlating with the previous works of Tang *et al.* and Zhang and his co-workers [16, 17].

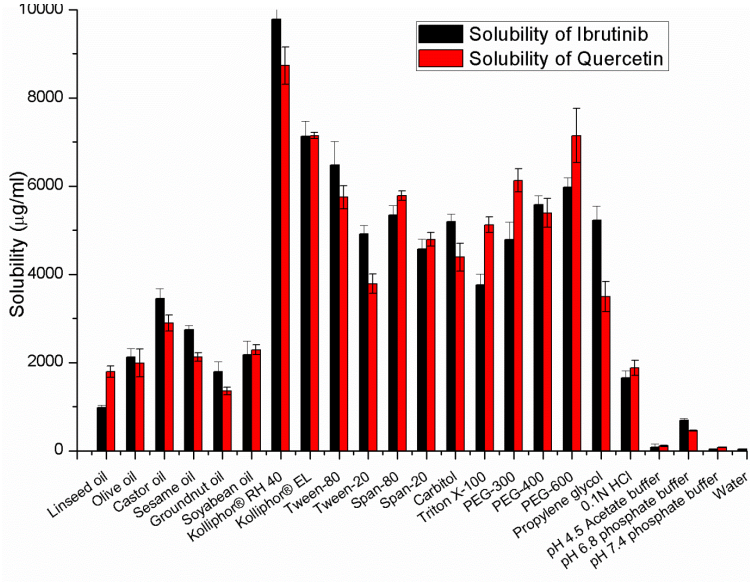

Fig. 1: Solubility of ibrutinib and quercetin in various oils and other solvents, Each value represents the mean±SD (n = 3)

Pseudo-ternary phase diagram

A large nano-emulsion area indicates better emulsification efficacy of the surfactant toward oil. For Kolliphor® RH 40/PEG-600 systems, they showed that increasing the Kolliphor® RH 40 to PEG-600 ratio increased the nano-emulsion area, which was explained by the increase in surfactant adsorption at the emulsion interface leading to decreases in surface tension and formulation droplet sizes. As seen in fig. 2, the green region of the diagram represented the efficient self-nanoemulsifying region. Based on this diagram, the range of each component was selected as follows: 54% ≤ Castor oil ≤ 60%, 24% ≤ Kolliphor® RH 40 ≤ 36%, 10% ≤ PEG-600 ≤ 20%.

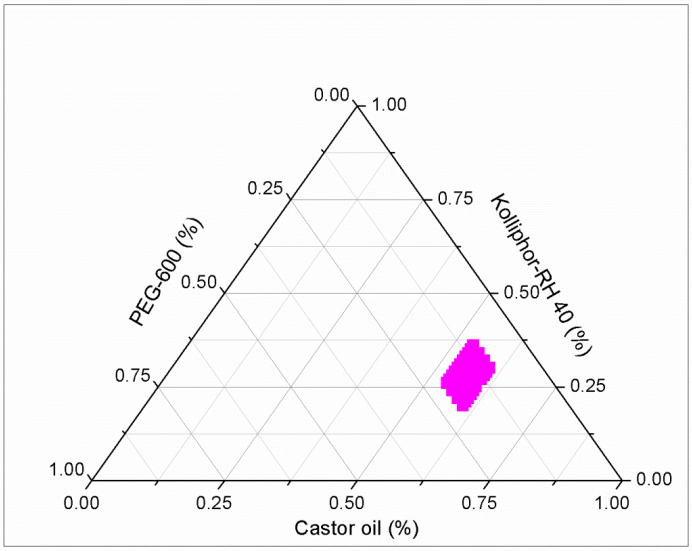

Fig. 2: Ternary phase diagram of dual drug-loaded SNEDDS

Design of experiments

The experiments were conducted as for the design and the obtained responses for the dependent variables droplet size (Y_1), encapsulation efficiency of ibrutinib (Y_2), and encapsulation efficiency of quercetin (Y_3) were presented in table 2. The design summary is as shown in fig. 3 [18].

Statistical analysis of the designed experiment

The range of droplet side (Y_1) for all batches was 70.18–200.56 nm. Similarly, the range for encapsulation efficiency of ibrutinib (Y_2) was 61.56–87.22 % and the range of encapsulation efficiency of quercetin (Y_3) was in the range 60.12–87.12 %. All three responses were fitted to a second quadratic model and the adequacy of this model was verified by ANOVA, lack of fit and multiple correlation coefficient (R^2) tests provided by Design-Expert software (table 3).

Table 3: Regression equations for the responses-particle size, polydispersity index and percent drug release after 15 min

Response	Regression equation
Y_1	77.80+30.11 A–5.87 B-25.30 C+6.82 BC+61.95 A^2+13.87 B^2+4.37 C^2
Y_2	85.94-3.08 A+6.08 B+4.71 C-2.05 AB-1.87 AC-2.93 BC-9.98 A^2-7.13 B^2
Y_3	86.31-2.60 A+5.45 B+5.48 C-4.15 AB-1.60 BC-10.53 A2-8.74 B2

The particle size of the nanoparticles was found to be in the range of 70.18–200.56 nm as shown in table 2.

The perturbation plot (fig. 4) showing the main effects of A, B and C on the droplet size (Y_1). The interaction between B and C on droplet size at a fixed level of A is shown in fig. 5. The respective contour plot is as shown in fig. 6.

Design Summary

Study Type	Response Surface	**Runs**	17
Design Type	Box-Behnken	**Blocks**	No Blocks
Design Model	Quadratic	**Build Time (ms)**	2.05

Factor	Name	Units	Type	Subtype	Minimum	Maximum	-1 Actual	+1 Actual	Mean	Std. Dev
A	Amount of castor oil	mg	Numeric	Continuous	54.00	60.00	54.00	60.00	57.00	2.06
B	Amount of Kolliphor RH 40	mg	Numeric	Continuous	24.00	36.00	24.00	36.00	30.00	4.12
C	Amount of PEG-600	mg	Numeric	Continuous	10.00	20.00	10.00	20.00	15.00	3.43

Response	Name	Units	Obs	Analysis	Minimum	Maximum	Mean	Std. Dev.	Ratio	Trans	Model
Y1	Droplet size	nm	17	Polynomial	70.18	200.56	115.535	43.7031	2.85779	None	No model chosen
Y2	Encapsulation efficiecny Ibrutinib	%	17	Polynomial	61.56	87.22	77.8865	8.98159	1.41683	None	No model chosen
Y3	Encapsulation efficiency Quercetin	%	17	Polynomial	60.12	87.12	77.2376	9.5164	1.4491	None	No model chosen

Fig. 3: The summary of box–behnken design

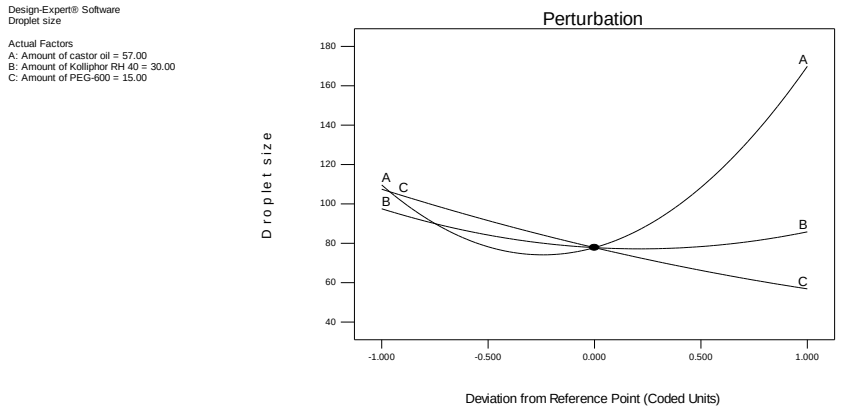

Fig. 4: Perturbation plot showing the effect of A, B and C on droplet size

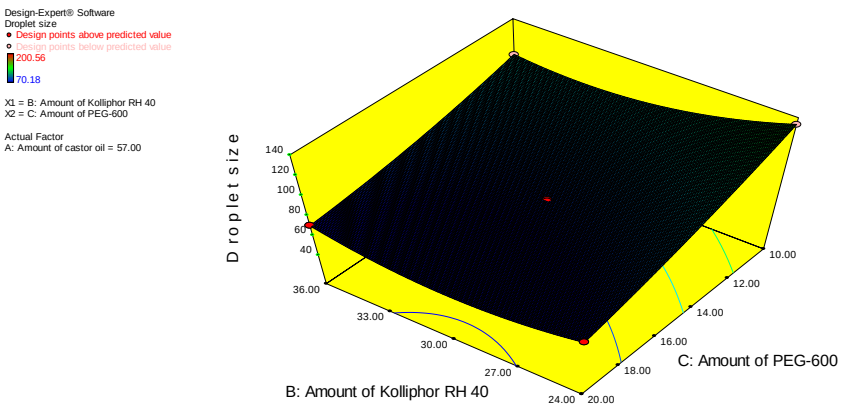

Fig. 5: Response surface plot showing the influence of B and C at fixed level of A

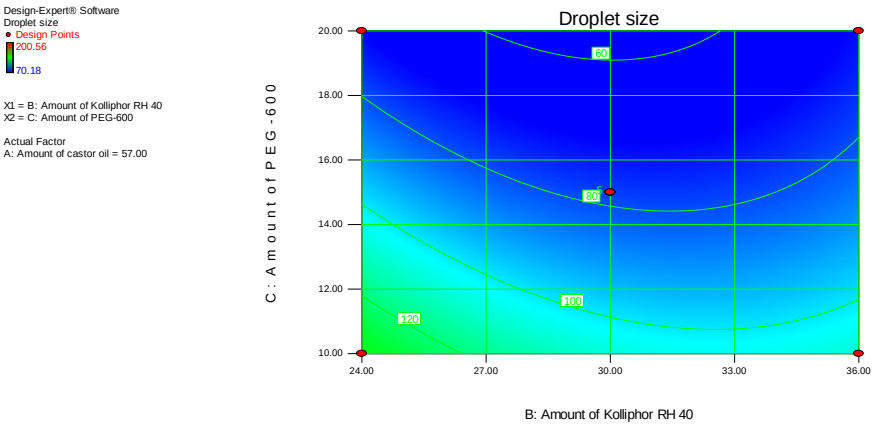

Fig. 6: Contour plot showing the influence of B and C at fixed level of A

Encapsulation efficiency of ibrutinib

The encapsulation efficiency of ibrutinib within the self-nano-emulsifying drug delivery system (SNEDDs) was evaluated, and the results, ranging from 61.56% to 87.22%, are presented in table 2. Fig. 7, known as the perturbation plot, illustrates the main effects of factors A, B, and C on the encapsulation efficiency of ibrutinib (Y2). It provides a visual representation of how each factor individually influences the encapsulation efficiency. Moving on to fig. 8, it showcases the interaction between factors A and B on the encapsulation efficiency of ibrutinib at a fixed level of factor C. The corresponding contour plot, presented in fig. 9, offers a graphical representation of this interaction. Similarly, fig. 10 demonstrates the interaction between factors A and C at a fixed level of factor B, accompanied by the respective contour plot in fig. 11. Additionally, fig. 12 depicts the interaction between factors B and C on the encapsulation efficiency of ibrutinib when factor A is fixed, while the contour plot for this interaction is shown in fig. 13. Together, these fig. and contour plots provide comprehensive insights into the relationships and interactions among factors A, B, and C regarding the encapsulation efficiency of ibrutinib within the SNEDDs, aiding in the analysis and optimization of the drug delivery system for enhanced efficiency.

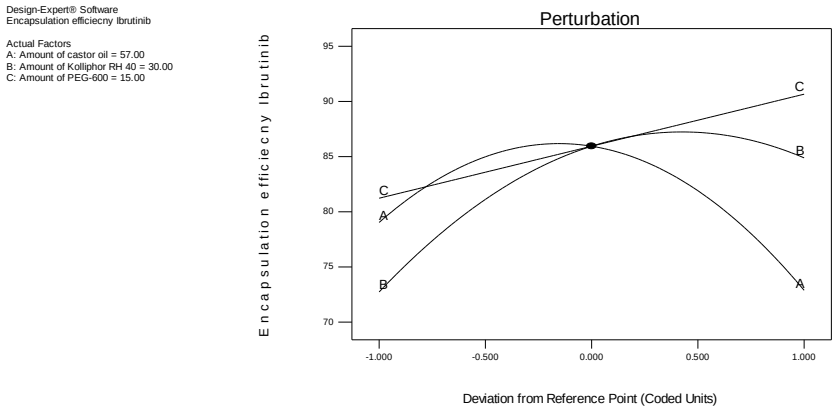

Fig. 7: Perturbation plot showing the effect of A, B and C on encapsulation efficiency of ibrutinib

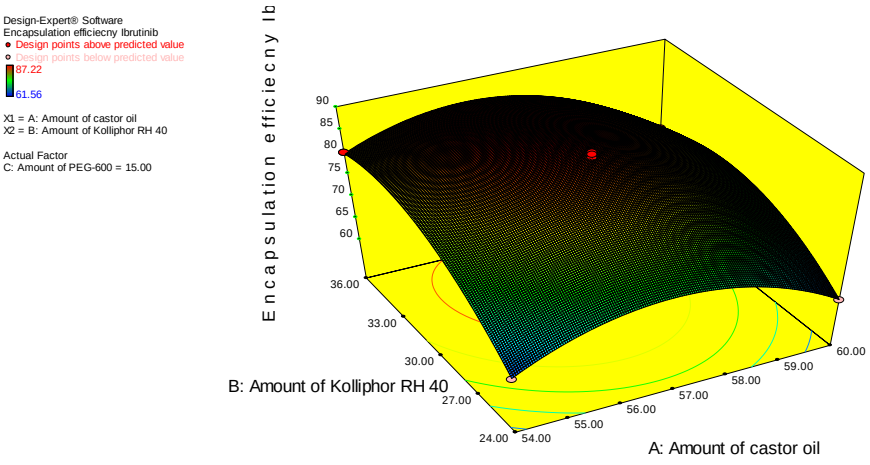

Fig. 8: Response surface plot showing the influence of A and B at fixed level of C

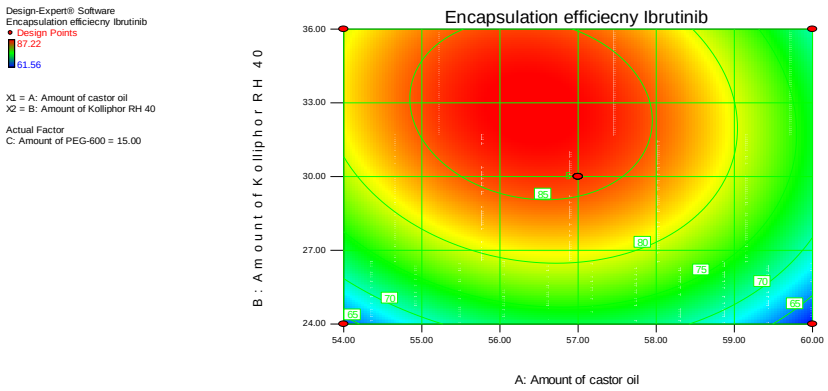

Fig. 9: Contour plot showing the influence of A and B at a fixed level of C

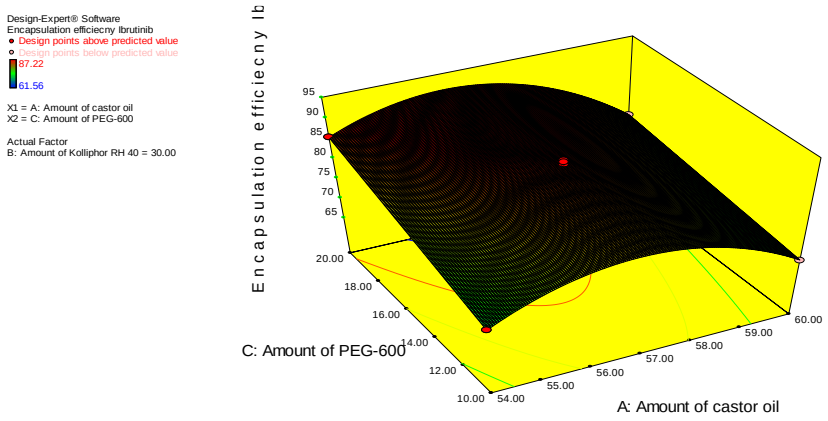

Fig. 10: Response surface plot showing the influence of A and C at fixed level of B

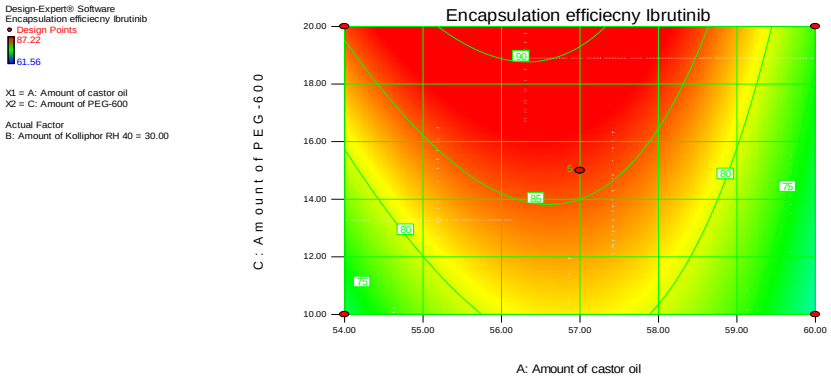

Fig. 11: Contour plot showing the influence of A and C at fixed level of B

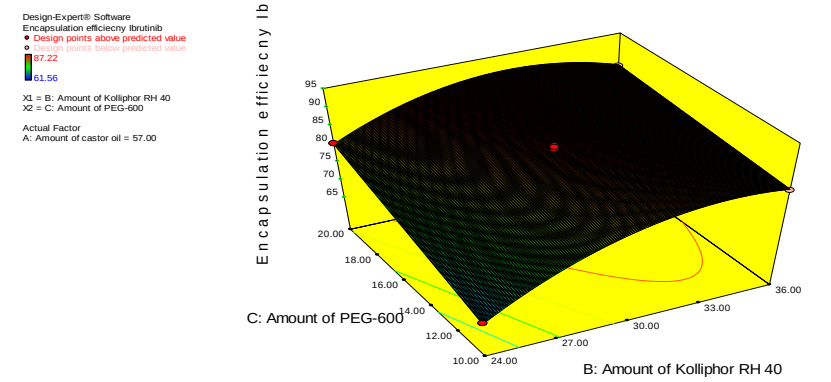

Fig. 12: Response surface plot showing the influence of B and C at fixed level of A

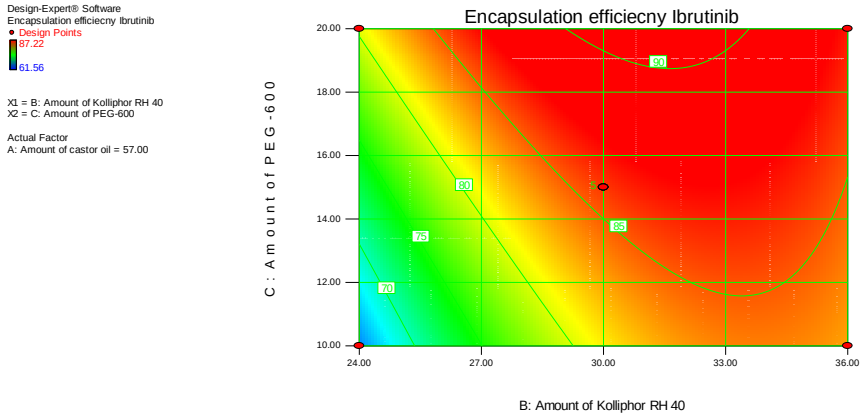

Fig. 13: Contour plot showing the influence of B and C at fixed level of A

Encapsulation efficiency of quercetin

The encapsulation efficiency of quercetin within the self-nano-emulsifying drug delivery system (SNEDDs) was assessed, with results ranging from 60.12% to 87.12% as presented in table 2. Fig. 14, known as the perturbation plot, illustrates the main effects of factors A, B, and C on the encapsulation efficiency of quercetin (Y2). This plot provides a visual representation of how each factor individually influences the encapsulation efficiency. Additionally, fig. 15 showcases the interaction between factors A and B on the encapsulation efficiency of quercetin at a fixed level of factor C, while the corresponding contour plot is presented in fig. 16. Similarly, fig. 17 depicts the interaction between factors B and C on the encapsulation efficiency of quercetin at a fixed level of factor A, accompanied by the respective contour plot in fig. 18. These fig. and contour plots provide comprehensive insights into the relationships and interactions among factors A, B, and C concerning the encapsulation efficiency of quercetin within the SNEDDs. The findings aid in the analysis and optimization of the drug delivery system, contributing to improved efficiency and performance.

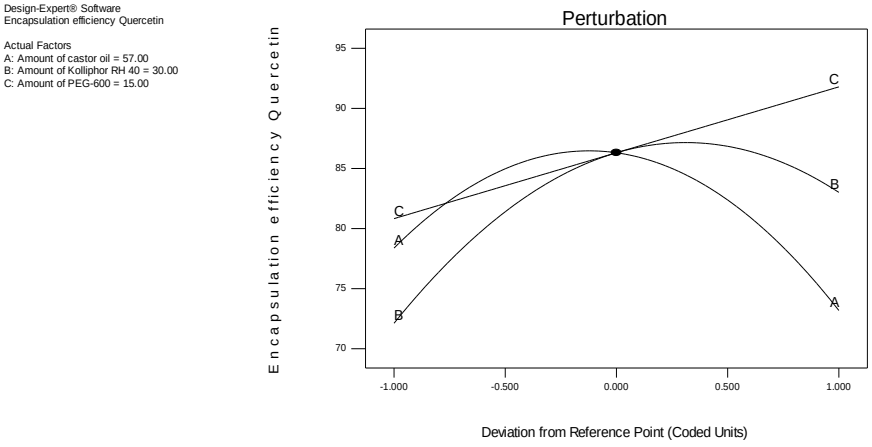

Fig. 14: Perturbation plot showing the effect of A, B and C on encapsulation efficiency of quercetin

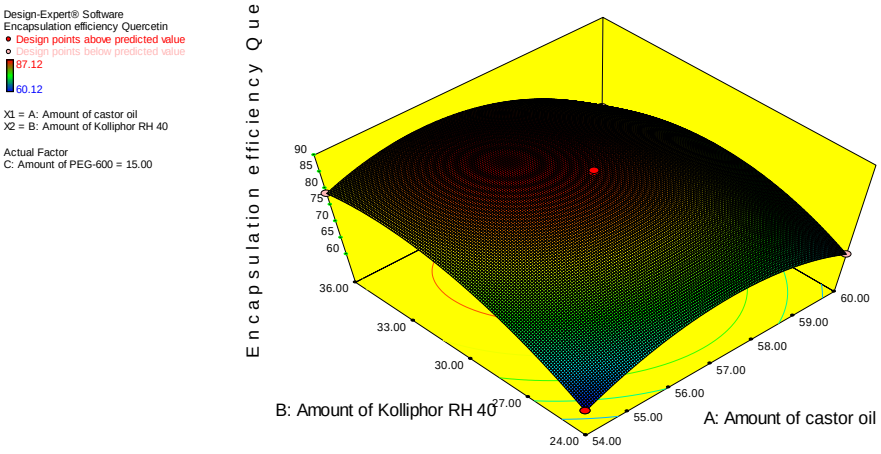

Fig. 15: Response surface plot showing the influence of A and B at fixed level of C

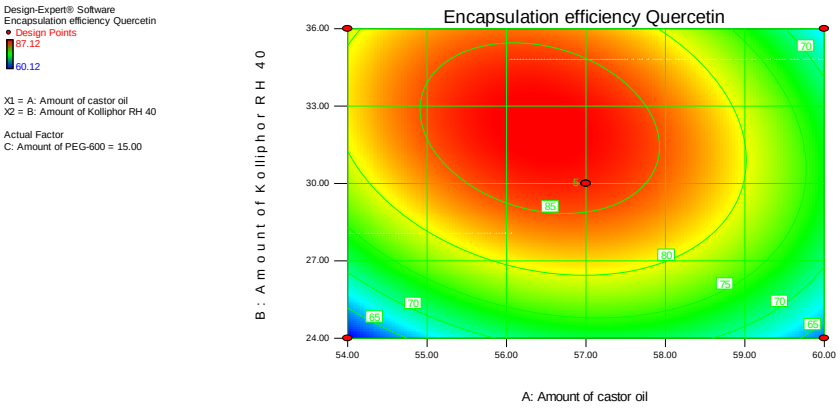

Fig. 16: Contour plot showing the influence of A and B at fixed level of C

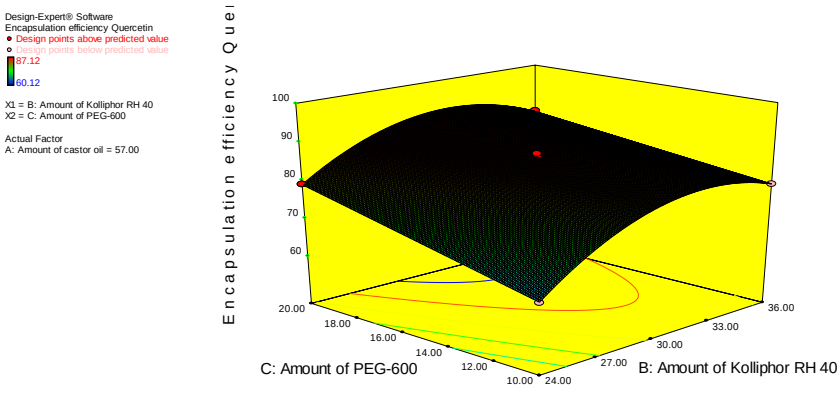

Fig. 17: Response surface plot showing the influence of B and C at fixed level of A

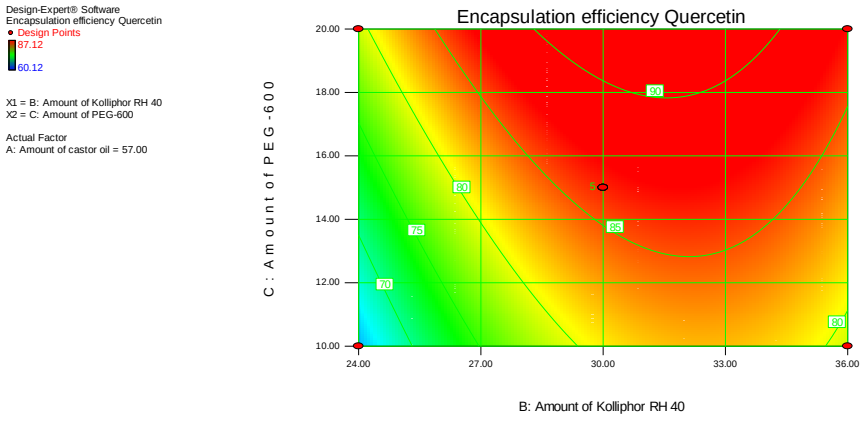

Fig. 18: Contour plot showing the influence of B and C at fixed level of A

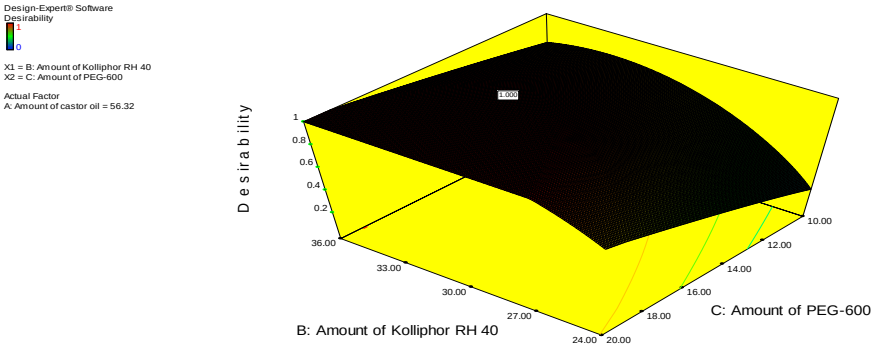

Fig. 19: 3D-response surface plot showing the global desirability value with point prediction

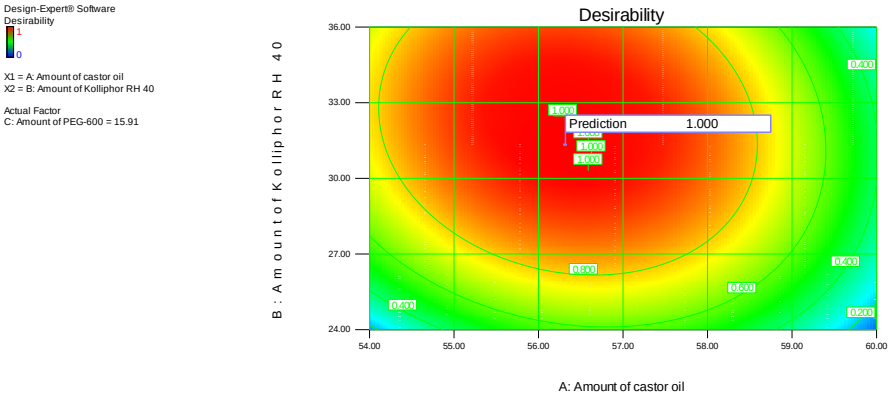

Fig. 20: Contour plot showing the global desirability value with point prediction

Table 4: Optimized values obtained by the constraints applies on Y_1, Y_2 and Y_3

Independent variable	Nominal values	Predicted values			Observed values			
		Droplet size (Y_1) (nm)	Encapsulation efficiency of ibrutinib (Y_2)	Encapsulation efficiency of quercetin (Y_3)	Batch	Droplet size (Y_1) (nm)	Encapsulation efficiency of ibrutinib (Y_2)	Encapsulation efficiency of quercetin (Y_3)
Amount of castor oil	56.32 mg	69.32	88.03	88.27	S1	75.34±4.24	87.24±1.86	88.12±3.28
Amount of Kolliphor® RH 40	31.32 mg				S2	76.38±5.26	86.54±2.25	87.58±4.12
Amount of PEG-600	15.91 mg				S3	71.12±3.14	85.68±3.17	86.59±1.39

(All determinations were performed in triplicate and values were expressed as mean±SD n=3)

Optimization by desirability function

The responses: droplet size (Y_1), encapsulation efficiency of ibrutinib (Y_2), and encapsulation efficiency of quercetin (Y_3) were transformed into the desirability scale, respectively. Among them, Y_1 has to be minimized, while Y_2 and Y_3 have to be maximized. For individual desirability function, Y_{max} and Y_{min} were taken as the highest objective function (D) was calculated by Equation (3) for each response. The prediction model is as shown in fig. 19 and 20 (table 4).

Evaluation of SNEDDS

Droplet size, polydispersity index and zeta potential

The droplet size for dual drug-loaded SNEDDS (S1-S3) ranged from 71.12-76.38 nm with PDI 0.126-0.312. The negative value of zeta potential ranging between-24.6 to-28.4 mV might be due to the presence of anionic groups of free fatty acids and glycols present in the oil, surfactant and co-surfactant [19, 20]. The particle size and zeta potential values were presented in table 5.

Table 5: Droplet size, polydispersity index and zeta potential of S-SNEDDS formulations

Sample	Particle size±SD (nm)	Polydispersity Index	Zeta potential (mV)
S1	75.34±4.24	0.193±0.005	-24.6±2.1
S2	76.38±5.26	0.126±0.005	-25.8±1.6
S3	71.12±3.14	0.312±0.005	-28.4±2.3

(All determinations were performed in triplicate and values were expressed as mean±SD, n=3)

Thermodynamic stability studies

The selected formulation passed the thermodynamic stability studies without any signs of phase separation and precipitation during alternative temperature cycles (4 °C and 40 °C), freeze-thaw cycles (-21 °C and+25 °C) and centrifugation at 3500, indicating good stability of the formulation.

Physicochemical characterization

The interactions between the drugs and other components were determined by FT-IR spectroscopy. The characteristic peaks of ibrutinib are seen at 3396.76, 1741.78, 1687.77, 1587.47, 1500.67, 1462.09, 1375.29, 1244.13, 1155.4, 1033.88, 972.16, 835.21, 746.48 and 704.04 cm^{-1}. Similarly, the characteristic peaks of quercetin are seen at 3406, 3283, 1666, 1610, 1560, 1510, 1379, 1317, 1263, 1200, 1165, 933, 820, 679 and 600 cm^{-1}. It is anticipated that ibrutinib and quercetin peaks were masked by the formulation absorption peaks due to the encapsulation of drug molecules within the SNEDDs (fig. 21).

In the XRPD pattern of the dual drug-loaded SNEDDS was completely amorphous, lacking characteristic peaks of both drugs (fig. 22).

DSC curves of ibrutinib, quercetin and SNEDDs formulation are shown in drugs have shown sharp endothermic peaks (figure). However, the SNEDDs formulation showed no specific peaks from 40 °C to 400 °C. This confirms that both drugs are presented in an amorphous form within the SNEDDS (fig. 23).

Scanning electron microscopy (SEM)

Scanning electron microscopy (SEM) studies showed that the regular spherical shape and size of all the SNEDDS formulations, as shown in fig. 24.

***In vitro* dissolution studies**

The comparative dissolution profiles of pure ibrutinib, quercetin and SNEDDS formulations were carried out both in SGF and SIF as dissolution medium is presented in fig. 25. The dissolution profile shows that the SNEDDS showed faster drug release (>50 % in 240

min) when compared with both pure drug dispersions. Rapid drug dissolution from the SNEDDS may be due to low surface free energy of the self-emulsifying systems, which favours rapid emulsification by quick establishment of an interface between dissolution medium and oil. The improved dissolution can be attributed to the greater surface area of the nanosized globules, the transformation of the drugs physical state from low water-soluble crystalline form to a non-crystalline amorphous or disordered crystalline phase of a molecular dispersion in SNEDDS. The *in vitro* dissolution studies revealed that both drugs are hydrophobic, in particular, Quercetin showed negligible drug dissolution at both SGF and SIF environments. These data emphasize the need for enhancing oral quercetin delivery by proper formulation design. Interestingly, ibrutinib-Quercetin SNEDDS showed superior ($p<0.05$) dissolution enhancement of both drugs at SGF and SIF. This was owing to the efficient self-nano emulsification process that formed a favorable environment to maintain the drug solubilized, within the nano-sized oil droplets, upon exposure to GI fluids.

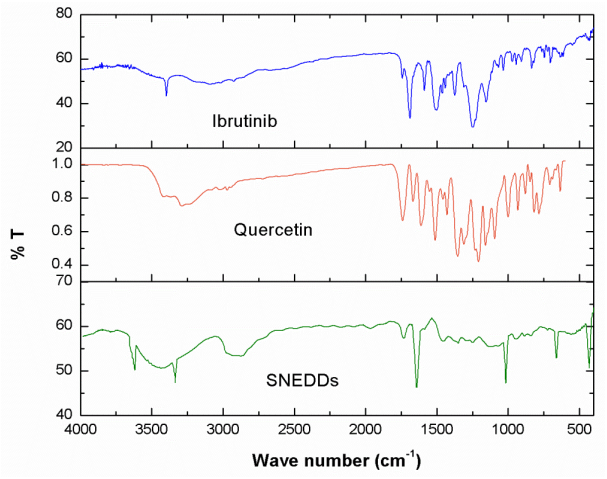

Fig. 21: FTIR spectra of pure ibrutinib, quercetin and SNEDDs formulation

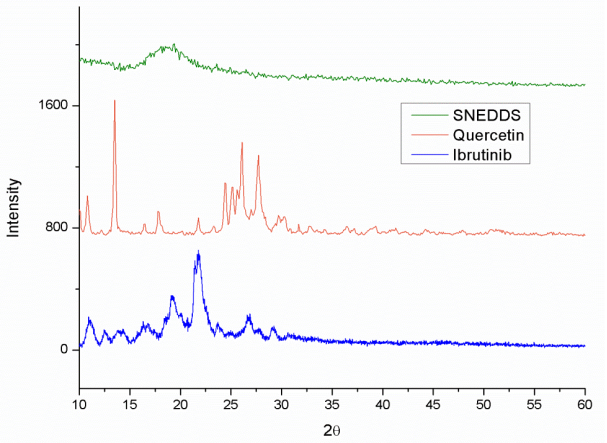

Fig. 22: XRD pattern of pure ibrutinib, quercetin and SNEDDs formulation

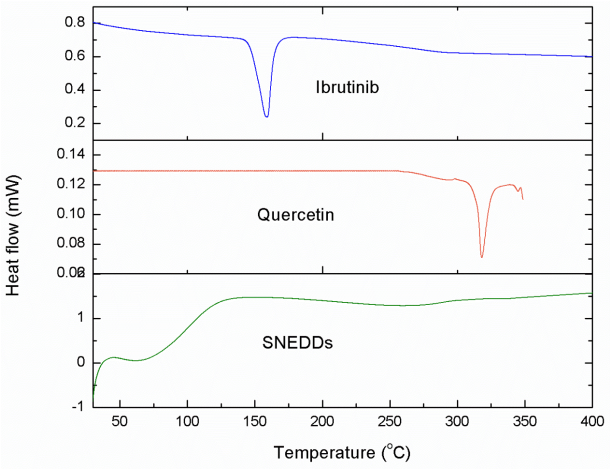

Fig. 23: DSC thermograms of pure ibrutinib, quercetin and SNEDDs formulation

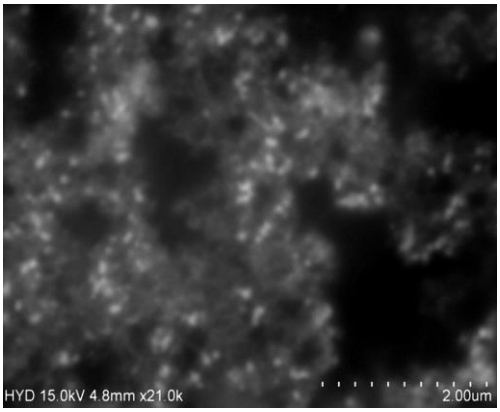

S1

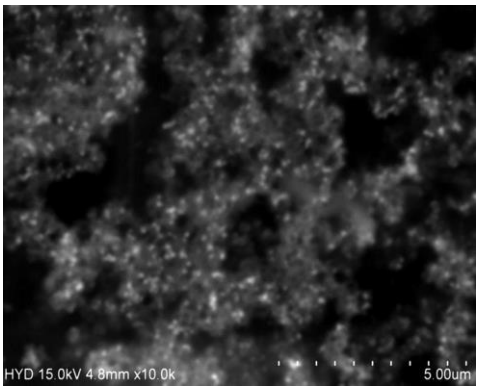

S2

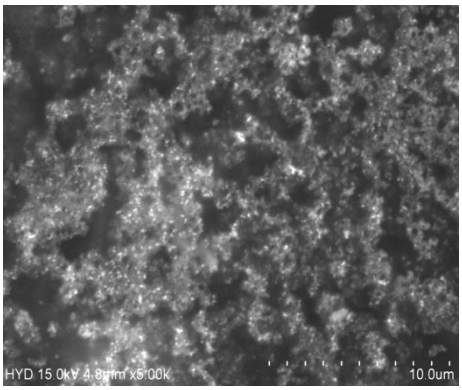

S3

Fig. 24: SEM images of SNEDDs formulations (S1, S2 and S3 under 21K, 10K and 5k magnification respectively)

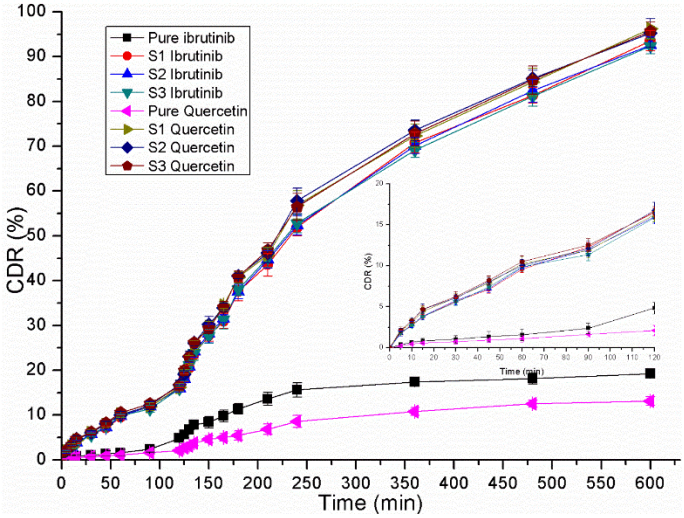

Fig. 25: Dissolution profile of ibrutinib and quercetin from SNEDDS formulations

Table 6: Droplet size, Zeta potential and PDI ibrutinib S-SNEDDS formulation after 90 d of storage at refrigerated and room temperature

Temperature	Particle size (nm)			Zeta potential			PDI		
(°C)	0 mo	3 mo	6 mo	0 mo	3 mo	6 mo	0 mo	3 mo	6 mo
4±1 °C	76.38±5.26	80.12±3.32	81.18±2.76	-25.8±1.6	-24.8±1.2	-26.2±2.4	0.126±0.005	0.158±0.005	0.182±0.005
25±2 °C	76.38±5.26	81.56±2.78	83.58±3.32	-25.8±1.6	-25.4±2.1	-24.9±2.7	0.126±0.005	0.166±0.005	0.196±0.005

(All determinations were performed in triplicate and values were expressed as mean±SD n=3)

Stability study

The purpose of stability testing is to provide evidence on how the quality of drug substance or drug product varies with time under the influence of a variety of environmental factors such as temperature, humidity and light. Table 6 indicates that no significant difference ($p<0.05$) was found in droplet size, zeta potential and PDI of optimized formulation stored at refrigerated conditions and at room temperature.

CONCLUSION

The combined dosage form of Ibrutinib-Quercetin SNEDDS formulation was successfully developed with increased drug Solubilization and enhanced dissolution rate. The formulation variables were optimized by response surface methodology. The optimized loaded formula consisted of 56.32 % Castor oil (oil; X1), 31.32 % Kolliphor® RH 40 (Surfactant; X2), and 15.91 % PEG-600 (Co-surfactant; X3) which formed aqueous thermodynamically stable nanoemulsion upon contact with aqueous medium without being affected by change in pH of media. *In vitro* release studies showed that the optimized formula had faster release than that of pure drugs, confirming the efficiency of SNEDDS for improving the solubility and dissolution rate of poorly water-soluble drugs (Ibrutinib/Quercetin) combination. *In vivo* studies proved the superior efficiency of optimized-SNEDDs to enhance oral bioavailability of Ibrutinib/Quercetin combination.

FUNDING

Nil

AUTHORS CONTRIBUTIONS

All authors have contributed equally.

CONFLICTS OF INTERESTS

Declared none

REFERENCES

1. Mokhtari RB, Homayouni TS, Baluch N, Morgatskaya E, Kumar S, Das B. Combination therapy in combating cancer. Oncotarget. 2017;8(23):38022-43. doi: 10.18632/oncotarget.16723.
2. Guo XY, Wang P, Du QG, Han S, Zhu SM, Lv YF. Paclitaxel and gemcitabine combinational drug-loaded mucoadhesive delivery system in the treatment of colon cancers. Drug Res. 2015;65(4):199-204. doi: 10.1055/s-0034-1375665.
3. Hassan S, Peluso J, Chalhoub S, Idoux Gillet Y, Benkirane Jessel N, Rochel N. Quercetin potentializes the respective cytotoxic activity of gemcitabine or doxorubicin on 3D culture of AsPC-1 or HepG2 cells, through the inhibition of HIF-1α and MDR1. PLOS ONE. 2020;15(10):e0240676. doi: 10.1371/journal.pone.0240676, PMID 33052979.
4. Aalipour A, Advani RH. Bruton's tyrosine kinase inhibitors and their clinical potential in the treatment of B-cell malignancies: focus on ibrutinib. Ther Adv Hematol. 2014 Aug;5(4):121-33. doi: 10.1177/2040620714539906, PMID 25360238.
5. Ghadi R, Dand N. BCS class IV drugs: highly notorious candidates for formulation development. Journal of Controlled Release. 2017;248:71-95. doi: 10.1016/j.jconrel.2017.01.014.
6. Reddy MR, Gubbiyappa KS. A systematic review on supersaturable self-nano emulsifying drug delivery system: a potential strategy for drugs with poor oral bioavailability. Int J App Pharm. 2022;14(3):16-33. doi: 10.22159/ijap.2022v14i3.44178.
7. Gottemukkula LD, Sampathi S. SNEDDS as lipid-based nanocarrier systems: concepts and formulation Insights. Int J App Pharm. 2022;14(2):1-9. doi: 10.22159/ijap.2022v14i2.42930.
8. Wang L, Dong J, Chen J, Eastoe J, Li X. Design and optimization of a new self-nano emulsifying drug delivery system. J Colloid Interface Sci. 2009;330(2):443-8. doi: 10.1016/j.jcis.2008.10.077, PMID 19038395.
9. Gupta S, Chavhan S, Sawant KK. Self-nano emulsifying drug delivery system for adefovir dipivoxil: design, characterization, *in vitro* and ex vivo evaluation. Colloids and Surfaces A: Physicochemical and Engineering Aspects. 2011;392(1):145-55. doi: 10.1016/j.colsurfa.2011.09.048.
10. Craig D. An investigation into the mechanisms of self-emulsification using particle size analysis and low-frequency dielectric spectroscopy. International Journal of Pharmaceutics. 1995;114(1):103-10. doi: 10.1016/0378-5173(94)00222-Q.
11. Date A, Nagarsenker M. Design and evaluation of self-nanoemulsifying drug delivery systems (SNEDDS) for cefpodoxime proxetil☆. International Journal of Pharmaceutics. 2007;329(1-2):166-72. doi: 10.1016/j.ijpharm.2006.08.038.
12. Sapiun Z, Imran AK, Rosmala Dewi ST, Masita Pade DF, Ibrahim W, Tungadi R. Formulation and characterization of self nano-emulsifying drug delivery system (snedds) fraction of N-hexane: ethyl acetate from sesewanua leaf (*Clerodendrum fragrans* Wild.). Int J App Pharm. 2023;15(2):72-7. doi: 10.22159/ijap.2023v15i2.46365.
13. Nazzal S, Khan MA. Response surface methodology for the optimization of ubiquinone self-nano emulsified drug delivery system. AAPS PharmSciTech. 2002;3(1):23-31. doi: 10.1208/pt030103.
14. Derringer G, Suich R. Simultaneous optimization of several response variables. J Qual Technol. 1980;12(4):214-9. doi: 10.1080/00224065.1980.11980968.
15. Kallakunta VR, Bandari S, Jukanti R, Veerareddy PR. Oral self emulsifying powder of lercanidipine hydrochloride: formulation and evaluation. Powder Technol. 2012;221:375-82. doi: 10.1016/j.powtec.2012.01.032.
16. Tran TH, Guo Y, Song D, Bruno RS, Lu X. Quercetin-containing self-nano emulsifying drug delivery system for improving oral bioavailability. J Pharm Sci. 2014;103(3):840-52. doi: 10.1002/jps.23858, PMID 24464737.
17. Zhang P, Liu Y, Feng N, Xu J. Preparation and evaluation of self-micro emulsifying drug delivery system of oridonin. Int J Pharm. 2008;355(1-2):269-76. doi: 10.1016/j.ijpharm.2007.12.026, PMID 18242895.
18. Shukla M, Jaiswal S, Sharma A, Srivastava PK, Arya A, Dwivedi AK. A combination of complexation and self-nano emulsifying drug delivery system for enhancing oral bioavailability and anticancer efficacy of curcumin. Drug Dev Ind Pharm. 2017;43(5):847-61. doi: 10.1080/03639045.2016.1239732, PMID 27648633.
19. El-Zahaby SA, AbouGhaly MHH, Abdelbary GA, El-Gazayerly ON. Zero-order release and bioavailability enhancement of poorly water-soluble vinpocetine from self-nano emulsifying osmotic pump tablet. Pharm Dev Technol. 2018;23(9):900-10. doi: 10.1080/10837450.2017.1335321, PMID 28540754.
20. Dash RN, Mohammed H, Humaira T, Reddy AV. Solid supersaturatable self-nano emulsifying drug delivery systems for improved dissolution, absorption and pharmacodynamic effects of glipizide. J Drug Deliv Sci Technol. 2015;28:28-36. doi: 10.1016/j.jddst.2015.05.004.